Excitation of anti-symmetric coupled spoof SPPs in 3D SIS waveguides based on coupling*

Li-li Tian(田莉莉)[1], Yang Chen(陈杨)[2], Jian-long Liu(刘建龙)[1], Kai Guo(郭凯)[1], Ke-ya Zhou(周可雅)[1], Yang Gao(高扬)[3], and Shu-tian Liu(刘树田)[1,†]

[1] *Department of Physics, Harbin Institute of Technology, Harbin* 150001, *China*
[2] *School of Electrical Enginnering & Information, Northeast Petroleum University, Daqing* 163318, *China*
[3] *College of Electronic Engineering, Heilongjiang University, Harbin* 150080, *China*

(Received 22 January 2016; revised manuscript received 7 March 2016; published online 9 June 2016)

According to the electromagnetic field distributions, there exist two kinds of coupled spoof surface plasmon polaritons (SSPPs), the symmetric and anti-symmetric modes, in the three-dimensional (3D) subwavelength spoof–insulator–spoof (SIS) waveguide. We study the dispersion and excitation of the two kinds of coupled SSPPs supported by the 3D SIS waveguide. The evolution of the dispersion with the thickness and gap width of the waveguide is numerically investigated, and we give a theoretical analysis according to the coupling mechanism. Specially, based on the coupling mechanism, we design a zipper structure, through which the excitation and propagation of the anti-symmetric coupled modes can be realized effectively.

Keywords: waveguides, surface plasmons, microwave technology

PACS: 84.40.Az, 73.40.Rw, 84.60.Bk, 75.40.Mg **DOI:** 10.1088/1674-1056/25/7/078401

1. Introduction

In ultraviolet, visible, and near-infrared frequency bands, metals are usually described by the Drude model and behave like plasma.[1] Coherent oscillation of conduction electrons near the surface of a metal gives rise to surface plasmon polaritons (SPPs), which propagate along the surface and are confined in the perpendicular direction.[2] Owing to their high spatial confinement of electromagnetic energy, SPPs have attracted a great deal of interest and have been applied to many fields in the last decade.[3–5] Sandwiching a thin insulator layer with two metallic claddings forms a metal–insulator–metal (MIM) waveguide.[6–9] In such an MIM waveguide, each single interface can sustain bound SPPs. When the two metal–insulator interfaces are close enough, the interaction between the SPPs will give rise to coupled SPPs. The coupled modes can be divided into symmetric and anti-symmetric ones according to the symmetry of their electromagnetic field distributions.[1,6,8] In far-infrared, terahertz, and microwave frequency bands, however, the metals behave like perfect electrical conductors (PECs). A metal–insulator interface cannot confine the surface electromagnetic waves effectively.[10,11] Although these waves can still propagate along the MIM waveguide, high attenuation occurs and limits the propagation distance.[12] If some corrugations, such as holes and grooves, are added to the metal–insulator interface, another surface electromagnetic wave, spoof SPPs (SSPPs), could be excited and confined at the interface.[13–17]

Among those corrugated interface structures, the one-dimensional arrays of subwavelength grooves have been widely studied for their remarkable structural simplicity.[15,18–20] Two such groove-array waveguides separated by an insulator gap symmetrically create a new waveguide, which is called a spoof–insulator–spoof (SIS) waveguide for its analog to the non-corrugated MIM waveguide.[21–23] Similarly, an SIS waveguide supports two kinds of coupled SSPPs, i.e., the symmetric and anti-symmetric modes. It is worth noting that the symmetry of the coupled modes has different definitions in the literature. For the coupled SPPs supported by the MIM waveguide in the visible regime, people always define the mode symmetry according to the electric field distributions,[1,7,8] while in the microwave and terahertz regions, the mode symmetry is usually defined according to the magnetic field distributions.[21–23]

Recently, Shen *et al.*[24,25] proposed that the dispersion of the SSPPs propagating along a three-dimensional (3D) groove-array waveguide is insensitive to the thickness of the waveguide. Their theoretical and experimental results demonstrated that the SSPPs are well confined in the perpendicular direction and can propagate long distances along arbitrarily curved ultrathin comb-shaped waveguides. Based on those discoveries, the 3D SIS waveguide has been proposed and investigated.[23,26–30] However, current researches mainly focus on one kind of the coupled modes.[26–28] If we consider their magnetic field distributions, the modes are symmetric ones. Recently, reference [30] proposed an effective method

*Project supported by the National Basic Research Program of China (Grant No. 2013CBA01702) and the National Natural Science Foundation of China (Grant Nos. 61377016, 61575055, 10974039, 61307072, 61308017, and 61405056).

†Corresponding author. E-mail: stliu@hit.edu.cn

© 2016 Chinese Physical Society and IOP Publishing Ltd

to excite the odd modes in the SIS waveguide. Actually, the odd modes in that literature are also symmetric ones. There is still no effective technique to excite the anti-symmetric modes defined by the magnetic field. In this work, we propose a coupling scheme and design a zipper structure. The anti-symmetric coupled SSPPs can be generated effectively in this structure.

2. Dispersion relations of coupled SSPPs

Figure 1(a) illustrates the diagram of a 3D groove-array waveguide, where d, w, and t are the period constant, width, and thickness of the waveguide, respectively. The geometric parameters of the groove include the depth h and width a. Such a comb-shaped waveguide supports highly confined SSPPs, whose behavior depends primarily on the geometry of the corrugations.[24,25] Two comb-shaped waveguides separated by a vacuum gap g symmetrically form a 3D SIS waveguide, as shown in Fig. 1(b). In the 3D SIS waveguide, each comb-shaped waveguide supports a certain SSPP. When the vacuum gap is small enough, the two SSPPs will interact with each other, resulting in the coupled SSPPs.

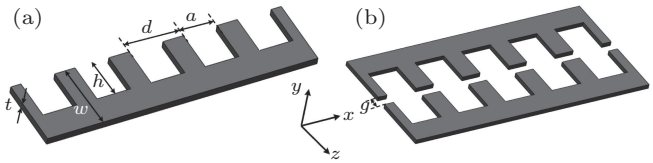


Fig. 1. (a) The structure sketch of a 3D groove-array waveguide. (b) The 3D SIS waveguide composed of two groove-array waveguides separated by a vacuum gap.

The case of coupled SSPPs propagating in a two-dimensional (2D) SIS waveguide has been analyzed in Ref. [21], which defined the symmetric/anti-symmetric modes based on the magnetic field distributions. In that paper, Kats *et al.* obtained rigorous dispersion relations of the two coupled modes numerically. According to the dispersion expressions, the symmetric modes converge to the zero frequency, while the anti-symmetric modes have cut-off frequencies; the anti-symmetric modes have higher eigen-frequencies than the symmetric modes.[21] In the following, we are concerned with the coupled SSPPs supported by the 3D SIS waveguide. With the purpose of comparing our results with those of the 2D case, we also define the symmetry of the coupled modes according to their magnetic field distributions. All the results are calculated using the finite integration method in this paper. We consider the microwave region and choose $d = 5$ mm as the length unit, then a, h, and w are fixed at $0.4d$, $0.8d$, and d, respectively. The metal is modeled as a PEC.

The influence of the waveguide thickness and gap width on the dispersion relations is investigated. Figure 2(a) illustrates the dispersion curves with respect to different waveguide thicknesses t, where the gap width g is fixed at 0.4 mm. The solid symbols denote the symmetric modes and the hollow ones denote the anti-symmetric modes. The black line is the light line, which represents the dispersion relation of the light in the vacuum. We can see that the dispersion curves of the symmetric modes are on the right of the light line, implying field confinement in the perpendicular direction, and they converge to the zero frequency. The dispersion curves of the anti-symmetric modes, which are above those of the symmetric modes, pass through the light line and enter the radiation region. These intersections with the light line correspond to the cut-off frequencies. All the features of both the symmetric and anti-symmetric modes agree with the coupled SSPPs supported by the 2D SIS waveguide.[21] As the thickness decreases, the two kinds of dispersion curves approach each other, which demonstrates that the interaction between the two SSPPs becomes weak. The reason is that the confinement of the SSPPs sustained by the comb-shaped waveguide becomes higher with the decrease of the waveguide thickness.[24,25] Figure 2(b) shows the evolution of the dispersion curves with the gap width g while the thickness t is fixed at 0.018 mm, which is one of the thicknesses of the printed circuit boards (PCB). As the gap width increases, the interaction of the SSPPs becomes weak. Therefore, the dispersion curves of the symmetric and anti-symmetric modes approach the dispersion curve of the comb-shaped waveguide simultaneously, which corresponds to the result when g takes infinite (marked by the red crosses).

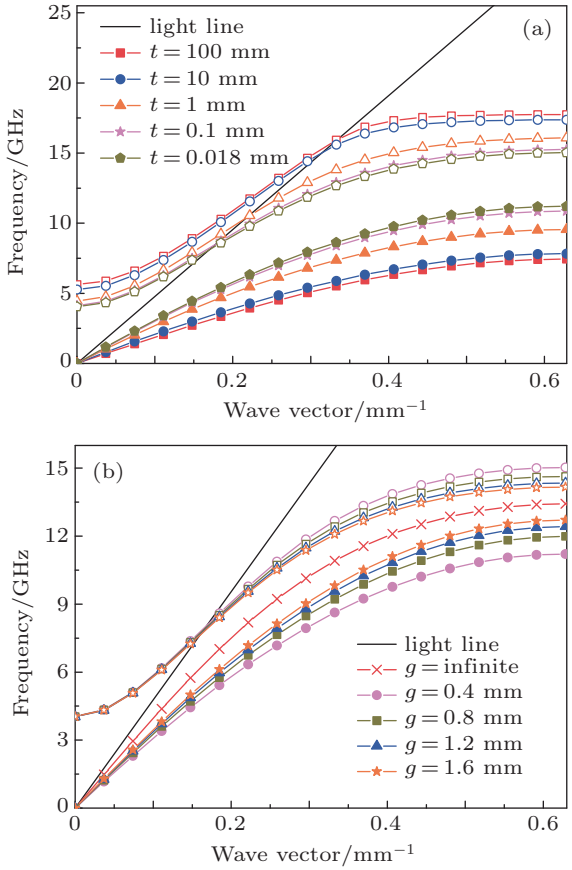


Fig. 2. (color online) Dispersion curves for the symmetric (solid symbols) and anti-symmetric (hollow symbols) coupled modes of the 3D SIS waveguide for (a) different thicknesses t with $g = 0.4$ mm and (b) different gap widths g with $t = 0.018$ mm. The black line is the light line. Here $d = 5$ mm, $a = 0.4d$, $h = 0.8d$, and $w = d$.

Figure 3 shows the electromagnetic profiles of the two kinds of coupled SSPPs. Figures 3(a) and 3(b) denote the H_y and E_y profiles of the symmetric coupled modes, while figures 3(c) and 3(d) show those of the anti-symmetric ones. The observation planes we chose are the central faces of the waveguides in the y direction. Interestingly, the symmetric modes have symmetric H_y distributions while their E_y distributions are anti-symmetric, and the anti-symmetric modes have anti-symmetric H_y and symmetric E_y distributions. That is why the symmetry of the coupled SSPPs has two definitions. From this point, the symmetric and anti-symmetric modes in this paper correspond to the odd and even modes in Ref. [30], respectively.

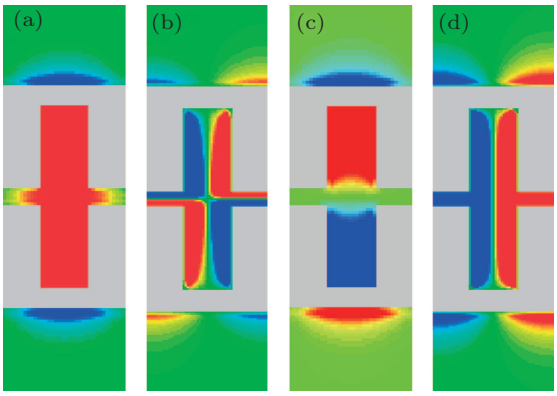


Fig. 3. (color online) The H_y and E_y profiles of a unit cell of the SIS waveguide for the coupled SSPPs: (a) H_y profile of the symmetric coupled mode, (b) E_y profile of the symmetric coupled mode, (c) H_y profile of the anti-symmetric coupled mode, (d) E_y profile of the anti-symmetric coupled mode.

3. Excitation and propagation of the anti-symmetric coupled SSPPs

Reference [30] designed a transducer using an asymmetric coplanar waveguide (CPW) and a slot line to excite the odd coupled SSPPs, that is, the symmetric modes, but the excitation of the anti-symmetric modes is still lacking. In the next, we introduce a zipper structure, through which the generation of the anti-symmetric coupled modes is realized. The zipper structure, designed on the base of the coupling scheme, also uses the property of the CPW.

The zipper structure proposed is divided into four regions, as shown in Fig. 4(a). Their horizontal lengths are 15 mm, 60 mm, 135 mm, and 180 mm in sequence. We fix the thickness of the waveguide at 0.018 mm and all the connection points are smooth. Region I is a CPW with the central bandwidth $w_{\mathrm{CPW}} = 30$ mm and slit width $g_{\mathrm{CPW}} = 0.4$ mm (as shown in Fig. 4(b)). Region II is a convertor composed of a piece of PEC plate and two gradient gratings. The boundary of the PEC plate is random as long as it has a similar shape with the one shown in Fig. 4(c). The depths of the grooves on the gradient gratings vary linearly from 0.4 mm to 4 mm. Region III consists of two curved comb-shaped waveguides. Both of them approach the x axis slowly and are parallel to each other in the right end with a gap width of 0.4 mm. Region IV is a 3D SIS waveguide. An RO4003 slice whose relative dielectric constant is 3.38 is used as the substrate. Its thickness is 0.058 mm. Ports 1 and 2 are the input and output ports, respectively.

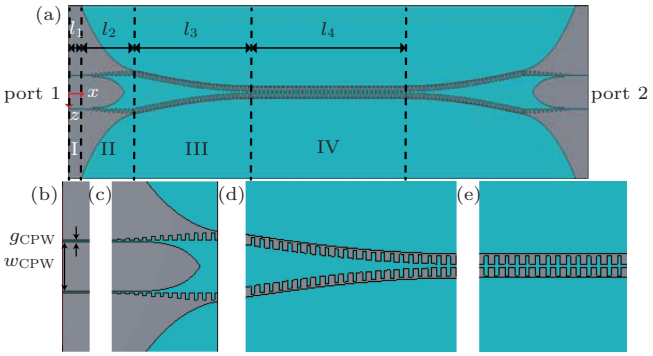


Fig. 4. (color online) (a) The top view of the zipper structure with an RO4003 substrate. (b)–(e) The enlarged view of regions I, II, III, and IV of the zipper structure.

In our design, regions I, II, III, and IV serve as the guided wave source, SSPPs convertor, SSPPs coupler, and propagation waveguide, respectively. An ungrounded CPW supports two guided modes. One is symmetric and the other is anti-symmetric. The symmetric (anti-symmetric) guided wave will convert to two symmetric (anti-symmetric) SSPPs lines when it transmits through region II. The gradient gratings in region II guarantee that the guided waves supported by the CPW convert to SSPPs gradually.[31,32] In region III, the two symmetric (anti-symmetric) transmission lines of SSPPs couple with each other gradually and form the symmetric (anti-aymmetric) coupled SSPPs in the end. The coupled SSPPs will propagate along the ultrathin SIS waveguide in region IV. However, it is noteworthy that the symmetric guided mode cannot transmit in the CPW naturally because its existence needs the electric symmetry condition. Only the anti-symmetric guided wave can propagate in the CPW without any symmetry conditions. It is a typical feature of the CPW. The electric symmetry condition is difficult to operate in practice. Therefore, the zipper structure is only effective to generate the anti-symmetric coupled SSPPs.

We use the finite integration method to simulate the whole excitation process. Figure 5 illustrates the spatial distributions of H_y and E_y in an xz plane, which is 0.5 mm above the surface of the zipper structure. The frequency takes 6 GHz in Figs. 5(a) and 5(b) and 10 GHz in Figs. 5(c) and 5(d). Such results can be attributed to two factors. The first one is that only an anti-symmetric guided wave exists in the CPW with the aid of the input port. The second one is that coupling two anti-symmetric SSPPs lines can generate anti-symmetric coupled modes, which is the mechanism of coupling. The H_y and E_y distributions of the whole structure show the generation and propagation of the anti-symmetric coupled modes vividly. It demonstrates the validity of our scheme.

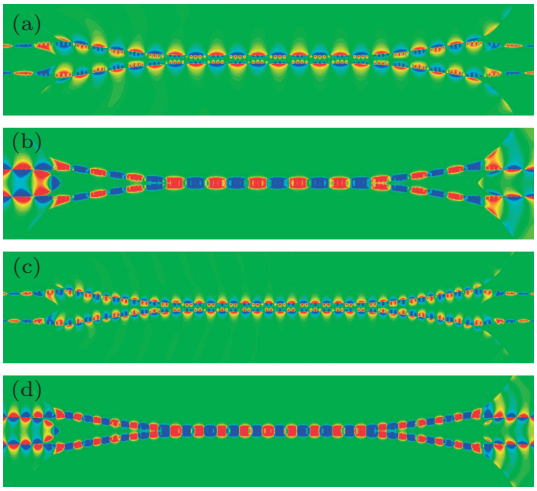


Fig. 5. (color online) The simulated electromagnetic field distributions in an xz plane, which is 0.5 mm above the surface of the zipper structure: (a) H_y distribution at 6 GHz, (b) E_y distribution at 6 GHz, (c) H_y distribution at 10 GHz, and (d) E_y distribution at 10 GHz.

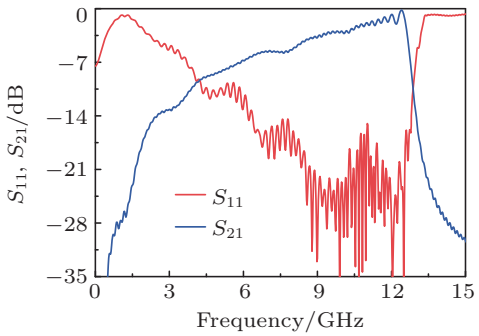


Fig. 6. (color online) The simulated S parameters of the zipper structure.

For an excitation system, it is necessary to check out its S parameters, which express the excitation efficiency. Figure 6 illustrates the simulated S parameters of the zipper structure. The S_{11} and S_{21} represent the reflection and transmission, respectively. We can obtain the working band of the zipper structure from the S parameters, which is from 4.3 GHz to 12.8 GHz. Especially, the zipper structure has a high excitation efficiency in the frequency range from 8.2 GHz to 12.6 GHz. The working band depends primarily on two factors. Firstly, the working frequencies have to satisfy the dispersion relations of the SSPPs supported by the comb-shaped waveguide. The reason is that the SSPPs will generate and propagate on the zipper structure. The dispersion relations of the SSPPs mainly decide the maximum working frequency. Secondly, the work frequencies are influenced by the dispersion relations of the coupled SSPPs since the coupled SSPPs must be able to propagate in region IV. They mainly decide the minimum working frequency. Additionally, the working band is also influenced by the substrate, but the influence is small here because the substrate used is very thin.

4. Conclusion

In a 3D SIS waveguide, both the symmetric and anti-symmetric modes have high confinement. But the applications of the SIS waveguide based on the anti-symmetric coupled modes are lacking because of the lack of excitation technique. We designed an ultrathin zipper structure with an inherent coupling mechanism that couples two SSPPs lines. In this structure, the anti-symmetric coupled SSPPs can be generated effectively. It is easy to conclude that the generation of the anti-symmetric coupled modes through the zipper structure is realizable in experiment. The scheme is simple, effective, and has the potential for further design of novel planar devices such as filters, resonators, and couplers.

References

[1] Maier S A 2007 *Plasmonics: Fundamentals and Applications* (1st Edn.) (New York: Springer) pp. 5–34
[2] Barnes W L, Dereux A and Ebbesen T W 2003 *Nature* **424** 824
[3] Fang N, Lee H, Sun C and Zhang X 2005 *Science* **308** 534
[4] Vedantam S, Lee H, Tang J, Conway J, Staffaroni M and Yablonovitch E 2009 *Nano Lett.* **9** 3447
[5] Lassiter J B, Sobhani H, Fan J A, Kundu J, Capasso F, Nordlander P and Halas N J 2010 *Nano Lett.* **10** 3184
[6] Dionne J A, Sweatlock L A, Atwater H A and Polman A 2006 *Phys. Rev. B* **73** 035407
[7] Feigenbaum E and Orenstein M 2007 *J. Lightw. Technol.* **25** 2547
[8] Pannipitiya A, Rukhlenko I D, Premaratne M, Hattori H T and Agrawal G P 2010 *Opt. Express* **18** 6191
[9] Wu C N, Li H J, Peng X, Gao G T amd Liu Z M 2013 *Chin. Phys. B* **22** 057301
[10] O'Hara J, Averitt R and Taylor A 2004 *Opt. Express* **12** 6397
[11] Saxler J, Rivas J G, Janke C, Pellemans H P M, Bolívar P H and Kurz H 2004 *Phys. Rev. B* **69** 155427
[12] Wang K L and Mittleman D M 2004 *Nature* **432** 376
[13] Pendry J B, Martin-Moreno L and Garcia-Vidal F J 2004 *Science* **305** 847
[14] Hibbins A P, Evans B R and Sambles J R 2005 *Science* **308** 670
[15] Garcia-Vidal F J, Martin-moreno L and Pendry J B 2005 *J. Opt. A: Pure Appl. Opt.* **7** S97
[16] Ding L, Liu J S and Wang K J 2010 *Chin. Phys. B* **19** 127302
[17] Gao Z, Shen L F, Wu J J, Yang T J and Zheng X D 2012 *Opt. Commun.* **285** 2076
[18] Shen L F, Chen X D and Yang T J 2008 *Opt. Express* **16** 3326
[19] Wang B W, Jin Y and He S 2008 *Appl. Opt.* **47** 3694
[20] Zhang j, Cai L K, Bai W L, Xu Y and Song G F 2009 *J. Appl. Phys.* **106** 103715
[21] Kats M A, Woolf D, Blanchard R, Yu N F and Capasso F 2011 *Opt. Express* **19** 14860
[22] Woolf D, Kats M A and Capasso F 2014 *Opt. Lett.* **39** 517
[23] Zhang Q, Xiao J J, Han D Z, Qin F F, Zhang X M and Yao Y 2015 *J. Phys. D: Appl. Phys.* **48** 205103
[24] Shen X P, Cui T J, Martin-Cano D and Garcia-Vidal F J 2013 *Proc. Nat. Acad. Sci. USA* **110** 40
[25] Shen X P and Cui T J 2013 *Appl. Phys. Lett.* **102** 211909
[26] Gao X, Shi J H, Shen X P, Ma H F, Jiang W X, Li L M and Cui T J 2013 *Appl. Phys. Lett.* **102** 151912
[27] Gao X, Zhou L, Liao Z, Ma H F and Cui T J 2014 *Appl. Phys. Lett.* **104** 191603
[28] Zhou Y J and Yang B J 2014 *Opt. Express* **22** 21589
[29] Quesada R, Martín-Cano D, Garcia-Vidal J and Bravo-Abad J 2014 *Opt. Lett.* **39** 2990
[30] Gao X, Zhou L and Cui T J 2015 *Sci. Rep.* **5** 9250
[31] Ma H F, Shen X P, Cheng Q, Jiang W X and Cui T J 2014 *Laser Phot. Rev.* **8** 146
[32] Liao Z, Zhao J, Pan B C, Shen X P and Cui T J 2014 *J. Phys. D: Appl. Phys.* **47** 315103